

AC conductivity studies and relaxation behaviour in $(\text{LiX})_y[(\text{Li}_2\text{O})_{0.6}(\text{P}_2\text{O}_5)_{0.4}]_{(1-y)}$ glasses

Thieu Duc Tho · Rayavarapu Prasada Rao · Stefan Adams

Received: 16 November 2009 / Revised: 7 May 2010 / Accepted: 10 May 2010 / Published online: 6 June 2010
© Springer-Verlag 2010

Abstract The electrical conductivity of $(\text{LiX})_y[(\text{Li}_2\text{O})_{0.6}(\text{P}_2\text{O}_5)_{0.4}]_{(1-y)}$ ($\text{X}=\text{Cl}, \text{Br}$, $y=0, 0.1, 0.15, 0.2$) glasses has been determined over a wide range of temperature and frequency by means of impedance spectroscopy. The real part of the frequency-dependent conductivity exhibits a simple power law feature, and the dimensionless frequency exponent n has been determined. The conductivity spectra show scaling behaviour when the conductivity spectra are scaled by $\omega/(\sigma_{dc}T)$ and ω/ω_p . The conductivity relaxation time and activation energy have been estimated from the modulus spectra. Increases of ionic conductivity values with addition of LiX content are in line with the decrease of activation energy and relaxation time.

Keywords Ionic conducting glasses · Transport properties · Impedance spectroscopy

Introduction

Lithium phosphate glasses possess technological importance because of their simple composition with strong glass-forming character and low glass transition temperature. With the addition of appropriate doping agent, these glasses find a wide variety of applications in optoelectronic devices and laser host materials and as solid electrolytes in solid-state ionic devices. Fast alkali ion conducting glasses with high ionic conductivity are potential candidates for applications in solid-state electrochemical devices such as

batteries, sensors, etc. due to their advantageous characteristics over the conventional crystalline materials.

A large number of reports are available on theoretical models to explain the ionic conduction mechanism in disordered solid electrolytes [1–6], emphasising the role of the shape and dynamic properties of the energy landscape predetermined by the local structure and composition of the glass. The commonly used models explain the conductivity from either microscopic hopping or macroscopic continuum models [2]. Hopping models are simple in approach and have been successfully adopted for a wide range of electron conducting, semiconducting and fast ion conducting systems. Especially, the random barrier model described by Dyre et al. [2] is found to explain ionic conduction characteristics as a hopping process in an energy landscape with a random distribution of energy barrier heights. Recently, we demonstrated the effect of modifying ion transport pathways by the addition of lithium halide (LiCl and LiBr) to the pure $(\text{Li}_2\text{O})_{0.6}(\text{P}_2\text{O}_5)_{0.4}$ glasses using a bond valence analysis of glass configurations generated by molecular dynamics simulations [7, 8]. In order to further understand the relaxation mechanism, here, we study the variation of dielectric constant with the addition of LiCl and LiBr to $(\text{Li}_2\text{O})_{0.6}(\text{P}_2\text{O}_5)_{0.4}$ glassy systems using frequency-dependent impedance spectroscopy.

Experimental details

Ternary glasses $(\text{LiX})_y[(\text{Li}_2\text{O})_{0.6}(\text{P}_2\text{O}_5)_{0.4}]_{(1-y)}$ (where $y=0, 0.1, 0.15, 0.20$, $\text{X}=\text{Cl}, \text{Br}$) were prepared by the conventional melt quenching method using $\text{NH}_4\text{H}_2\text{PO}_4$, Li_2CO_3 and LiX [7]. Appropriate amounts of $\text{NH}_4\text{H}_2\text{PO}_4$ and Li_2CO_3 were mixed, ground and kept in a platinum crucible at 300 °C for 30 min to get rid of NH_3 and H_2O and then

T. Duc Tho · R. Prasada Rao (✉) · S. Adams
Department of Materials Science and Engineering,
National University of Singapore,
Singapore 117574, Singapore
e-mail: mserpr@nus.edu.sg

Table 1 Composition analysis, E_a and fitting parameters of ac conductivity and modulus analysis

Nominal composition	Theor./wt _X (%)	Exp./wt _X (%)	Experimental composition	E_a^{dc} /(eV)	$E_a^{\omega_p}$ /(eV)	n	β
(Li ₂ O) _{0.60} (P ₂ O ₅) _{0.40}	—	—	(Li ₂ O) _{0.60} (P ₂ O ₅) _{0.40}	0.650	0.625	0.91	0.87
(Li ₂ O) _{0.54} (P ₂ O ₅) _{0.36} (LiCl) _{0.10}	4.96	4.87	(Li ₂ O) _{0.54} (P ₂ O ₅) _{0.36} (LiCl) _{0.098}	0.601	0.588	0.94	0.90
(Li ₂ O) _{0.51} (P ₂ O ₅) _{0.34} (LiCl) _{0.15}	7.61	7.14	(Li ₂ O) _{0.51} (P ₂ O ₅) _{0.34} (LiCl) _{0.141}	0.584	0.569	0.94	0.91
(Li ₂ O) _{0.48} (P ₂ O ₅) _{0.32} (LiCl) _{0.20}	10.39	10.26	(Li ₂ O) _{0.48} (P ₂ O ₅) _{0.32} (LiCl) _{0.198}	0.568	0.547	0.94	0.93
(Li ₂ O) _{0.54} (P ₂ O ₅) _{0.36} (LiBr) _{0.10}	10.52	10.13	(Li ₂ O) _{0.54} (P ₂ O ₅) _{0.36} (LiBr) _{0.096}	0.575	0.565	0.95	0.90
(Li ₂ O) _{0.51} (P ₂ O ₅) _{0.34} (LiBr) _{0.15}	15.66	15.65	(Li ₂ O) _{0.51} (P ₂ O ₅) _{0.34} (LiBr) _{0.150}	0.555	0.544	0.95	0.91
(Li ₂ O) _{0.48} (P ₂ O ₅) _{0.32} (LiBr) _{0.20}	20.72	20.59	(Li ₂ O) _{0.48} (P ₂ O ₅) _{0.32} (LiBr) _{0.199}	0.535	0.521	0.95	0.94

heated up to 700 °C for 2 h to remove CO₂ from the samples. The samples were melted for 30 min at 800 °C, and then an appropriate amount of LiX was added into the crucible, stirred to homogenise the melt and kept for 5 min. The melted glasses were then pressed between two copper plates preheated to 200 °C to avoid shattering of the glasses during quenching. The exact composition of the sample was determined from scanning electron microscopy with the aid of energy-dispersive X-ray analysis. Table 1 shows a comparison between expected and observed halide contents in the corresponding glasses. The samples were characterised by X-ray powder diffractometry using CuK α radiation (PANalytical X'Pert PRO) in the 2θ range 10° to 80° to confirm the glassy nature of samples. Ionic conductivity measurements for the temperature range of 300 to 492 K were carried out by impedance spectroscopy (*Schlumberger Solartron SI 1260*) in the frequency range of 1 Hz to 15 MHz; details are described elsewhere [7]. The frequency-dependent conductivity is fitted to an equivalent circuit model of one RC couple (representing the bulk resistance and geometric capacitance) in series with one CPE (representing polarisation at the electrode/electrolyte interface; Fig. 1).

Results and discussions

Impedance analysis

A series of Nyquist plots of (Li₂O)_{0.54}(P₂O₅)_{0.36}(LiBr)_{0.10} glass at different temperatures is shown in Fig. 1. Figure 2a then demonstrates that the DC ionic conductivity—as expected for the systems under investigation—follows the Arrhenius-type behaviour. The resulting activation energies, E_a^{dc} , are summarised in Table 1. The temperature-dependent complex impedance data of all the compositions have been analysed in the conductivity and electric modulus formalisms to shed light on conduction characteristics.

Frequency dependence of ionic conductivity

Analysis of the frequency dependence of ionic conductivity at various temperatures of the electrolytes helps to reveal insights into the hopping (jump) frequency of the ions, their temperature dependence, extrapolated DC conductivity and also whether the mobile ion concentration is thermally activated [8–11]. Figure 3 shows frequency-dependent conductivity plot of log(σ) versus log(ω) for the composition (Li₂O)_{0.54}(P₂O₅)_{0.36}(LiCl)_{0.10}. Three distinct regions in the conductivity spectra are observed for the compounds at above room temperatures: (1) the high-frequency dispersive region ($\omega > 10^4$ Hz); (2) the central plateau region, which is also called DC regime; and (3) the low-frequency dispersive region. The frequency dispersion characteristics in the high-frequency region can be analysed using Jonscher's universal power law relation,

$$\sigma(\omega) = \sigma(0) + A\omega^n \quad (1)$$

where $\sigma(0)$ is the frequency-independent DC conductivity of the sample, A is a weakly temperature-dependent quantity ($\approx 4 \times 10^{-11}$ for (Li₂O)_{0.6}(P₂O₅)_{0.4} glass and

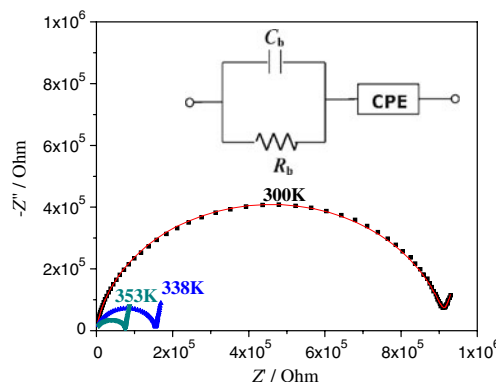
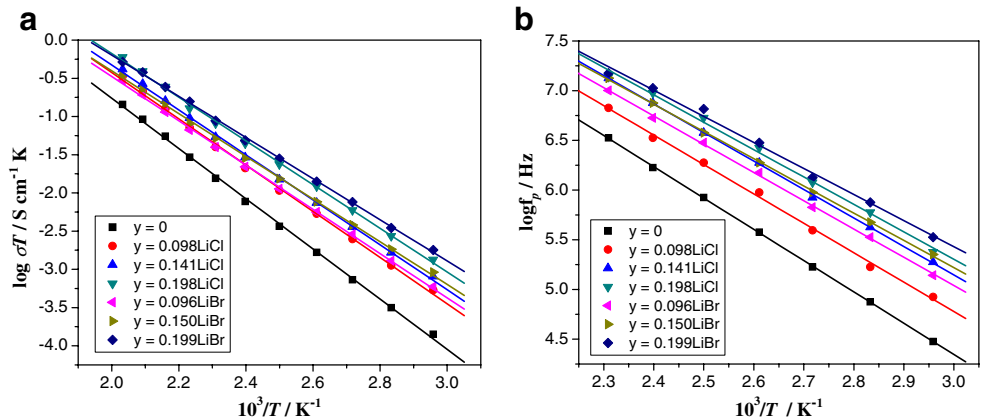


Fig. 1 Nyquist plots of (Li₂O)_{0.54}(P₂O₅)_{0.36}(LiBr)_{0.10} glass at different temperatures with equivalent circuit

Fig. 2 Arrhenius plot of **a** conductivity and **b** hopping frequency for all compositions



$\approx 3 \times 10^{-11}$ for LiX-doped glasses) and n is the power law exponent ($0 < n < 1$). As the temperature increases, the frequency at which the dispersion becomes prominent shifts to higher-frequency region, as the kinetic energy of the ions and hence their vibrational frequency increases (Fig. 3). The onset points of the conductivity dispersion at different temperatures lie on a straight line inclined at an angle of 45° (slope = 1) as shown in Fig. 3 for $(\text{Li}_2\text{O})_{0.54}(\text{P}_2\text{O}_5)_{0.36}(\text{LiCl})_{0.10}$. This suggests that DC conductivity $\sigma_{dc}(T)$ and onset frequency ω are proportional to each other and both are thermally activated with nearly the same activation energy, indicating a general feature of the power law proposed by Funke [12]. An analogous behaviour was observed when varying the content of LiX.

Scaling of AC conductivity data for ionically conducting glasses and amorphous semiconductors to construct a master curve in order to realise a common underlying behaviour was reported previously [13–16]. The AC conductivities obtained at different temperatures follow the relation,

$$\frac{\sigma(\omega)}{\sigma_{dc}} = F\left(\frac{\omega}{\omega_p}\right) \quad (2)$$

where F is a temperature-independent scaling function, and ω_p is the hopping frequency at which $\sigma = 2\sigma_{dc}$. The hopping frequency ω_p is found to increase with temperature (see Fig. 2b), LiX addition and halide size. For the same composition and temperature, ω_p of LiBr-doped glasses is higher than that of LiCl-doped glasses. The temperature dependence of ω_p obeys the Arrhenius behaviour. Also, as shown in Table 1, the hopping activation energies ($E_a^{\omega_p}$) are comparable to those of DC conductivity (E_a^{dc}). This suggests that the relaxation mechanism requires the charge carriers to cross the same energy barrier as for the conduction process [14]. Figure 4a shows the scaling of the AC conductivity spectra of $(\text{Li}_2\text{O})_{0.54}(\text{P}_2\text{O}_5)_{0.36}(\text{LiCl})_{0.10}$ at different temperatures. The value ω_p at various

temperatures obtained from frequency-dependent conductivity $\sigma(\omega)$ approximately follows the relation,

$$\sigma(\omega) = \sigma_{dc} \left[1 + \left(\frac{\omega}{\omega_p} \right)^n \right] \quad (3)$$

As the characteristic frequency is activated by the same thermal energy as $\sigma_{dc}T$, the scaling parameter can also be chosen as $\sigma_{dc}T$ instead of ω_p . The advantage of using this scaling parameter is that it employs the directly available quantities σ_{dc} and T rather than the value of ω_p that has to be derived from the conductivity dispersion. Figure 4b shows the same data as Fig. 4a with ω now scaled by $\sigma_{dc}T$. The exponent n in Eq. 3 is found to decrease slightly with increasing temperatures and to exhibit a minute increase with LiX content. The values of n observed for all compounds are $\sim 0.94 \pm 0.04$. Nearly the same values of n would follow from Eq. 1 (as n is close to 1). Since the Li-ion number densities of the investigated systems vary only slightly, the master curves for different glasses nearly fall on a super master curve (except for the low-frequency region) and it can hardly be decided whether the additional

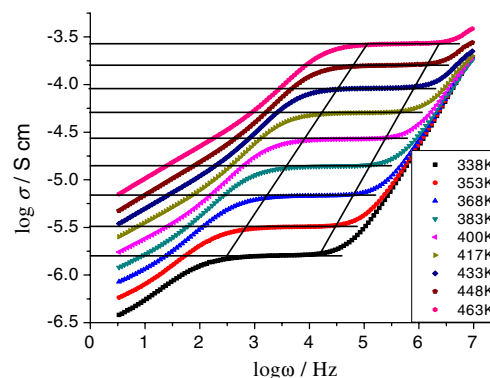


Fig. 3 Log-log plot of σ vs ω at different temperatures for $(\text{Li}_2\text{O})_{0.54}(\text{P}_2\text{O}_5)_{0.36}(\text{LiCl})_{0.10}$

Fig. 4 Conductivity master curves. **a** $\log(\sigma/\sigma_{dc})$ vs $\log(\omega/\omega_p)$; **b** $\log(\sigma/\sigma_{dc})$ vs $\log(\omega/\sigma_{dc}T)$ of $(\text{Li}_2\text{O})_{0.54}(\text{P}_2\text{O}_5)_{0.34}(\text{LiCl})_{0.10}$ at various temperatures

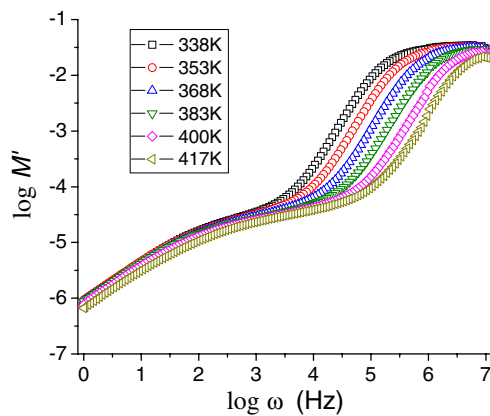
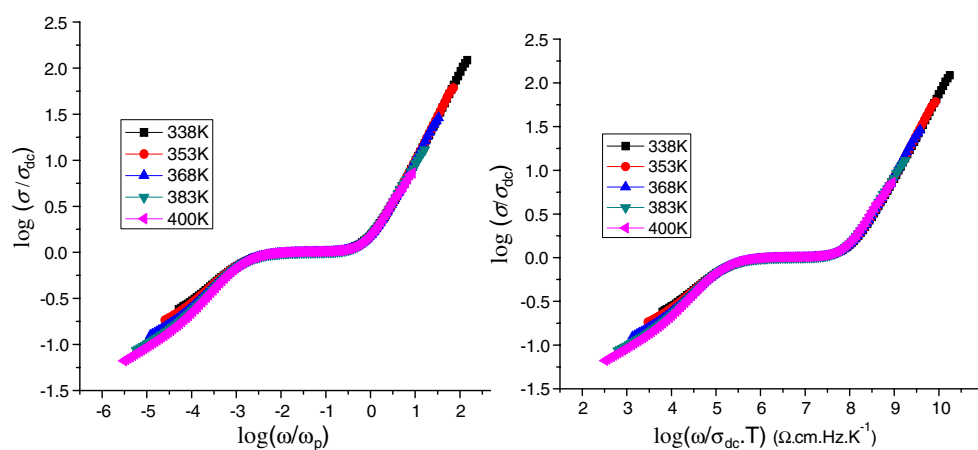


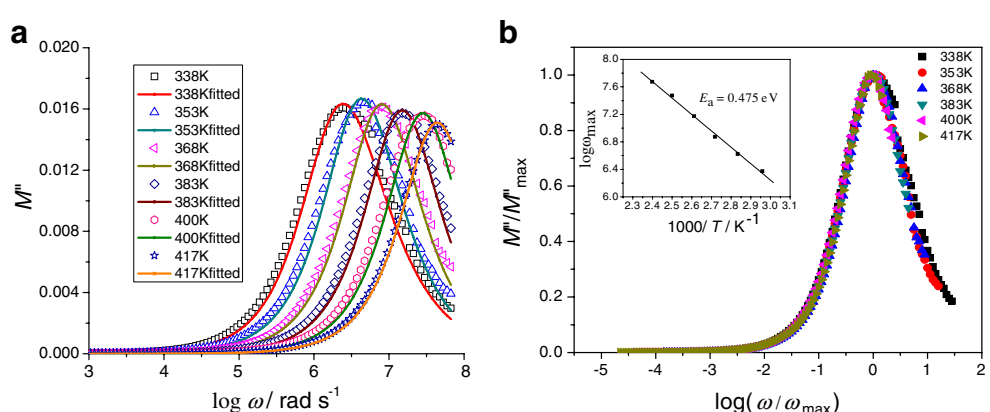
Fig. 5 Logarithmic variation of real part of modulus (M') with frequency (ω) for $(\text{Li}_2\text{O})_{0.51}(\text{P}_2\text{O}_5)_{0.34}(\text{LiBr})_{0.15}$ glass

scaling by the mobile ion concentration (as proposed by Roling et al. [3, 14]) improves the agreement among the curves. The low-frequency dispersion observed for compositions at various temperatures is due to the electrode polarisation as a result of the accumulation of mobile ions at the interface. The development of the space charge accumulation is more effective at lower frequencies [16]. Therefore, the total σ_{dc} of the compound decreases as frequency decreases at a given temperature. The drop in σ can be seen in Figs. 3 and 4 for frequencies below the middle plateau (DC) frequency regime. The dispersion is steeper and also the onset point of the low-frequency dispersion shifts to a higher frequency value with increasing temperature. This is due to the fact that the higher ion mobility at higher temperatures results in faster and more pronounced accumulation of ions and hence a corresponding drop in σ . As for high-frequency dispersion, the onset points of low-frequency dispersion at different temperatures lie on a straight line inclined at a slope of 0.83 (Fig. 3).

Modulus analysis

The analysis of impedance data in the modulus formalism assumes importance, as it suppresses the electrode effects in

Fig. 6 **a** Variation of imaginary part of modulus (M'') with frequency (ω) for $(\text{Li}_2\text{O})_{0.48}(\text{P}_2\text{O}_5)_{0.32}(\text{LiBr})_{0.20}$ glass. **b** Normalised plots (M''/M''_{max}) vs. $\log(\omega/\omega_{max})$ for $(\text{Li}_2\text{O})_{0.48}(\text{P}_2\text{O}_5)_{0.32}(\text{LiBr})_{0.20}$ glass. Inset: Arrhenius plot of peak frequencies ω_{max}



extracting the conductivity relaxation times. The electric modulus data can be obtained from the complex impedance data using the relation

$$M^* = M' + M'' = \frac{1}{\varepsilon} = j\omega C_0 Z^* \quad (4)$$

where C_0 is the vacuum capacitance and Z^* the complex impedance. Figure 5 shows the variation of the real part of electric modulus with frequency at different temperatures for $(\text{Li}_2\text{O})_{0.51}(\text{P}_2\text{O}_5)_{0.34}(\text{LiBr})_{0.15}$. At lower frequencies, M' tends to be very small, confirming that the electrode effects make a negligible contribution and hence may be ignored when the data are analysed in modulus formalism. For all temperatures, M' reaches a constant value $M_\infty (M_\infty = 1/e_\infty)$ at high frequencies, due to relaxation processes that spread over a range of frequencies. The M'' peaks are asymmetric and broader on both sides of the maxima than predicted by ideal Debye behaviour (Fig. 6). The frequency range where the peak occurs indicates the transition from long-range to short-range mobility. The peak in M'' shifts toward higher frequencies with increase in temperature. The asymmetric M'' plot is suggestive of stretched exponential character of relaxation times. The stretched exponential function is defined by the empirical Kohlrausch–Williams–Watts (KWW) function:

$$\phi(t) = \exp\left(-\frac{t}{\tau}\right)^\beta \quad (5)$$

where τ is the relaxation time and $0 < \beta < 1$ characterises the departure from a linear exponential behaviour ($\beta=1$). In fitting to Eq. 5, β and M_∞ have been taken as freely adjustable parameters at each temperature. The solid lines through the modulus spectra in Fig. 6 show the fits in good agreement with the experimental data. The average β value is found to depend on LiX content and temperature. The frequency exponent β does not obey Ngai's relation $\beta=1-n$ because the KWW function used for fitting the modulus spectra leaves the high-frequency component unaccounted, whereas the conductivity formalism takes it into account. The superimposed plots of M''/M''_{\max} vs $\log(\omega/\omega_{\max})$ suggest that the dynamical processes governing conductivity relaxations at different frequencies remain the same over the investigated temperature range (Fig. 6b). The temperature dependence of ω_{\max} obeys an Arrhenius relation $\omega_{\max} = \omega_0 \exp[-E_a/(kT)]$, where E_a is the activation energy for the electrical relaxation (cf. Fig. 6b). The values of E_a are

found to be comparable with the values obtained from temperature-dependent conductivity study.

Conclusions

AC conductivity and dielectric behaviour of $(\text{Li}_2\text{O})_{0.6}(\text{P}_2\text{O}_5)_{0.4}$ glass doped with LiX have been studied as a function of temperature and frequency. The frequency-dependent conductivity at different temperatures has been analysed using Jonscher's power law approach. The exponent n is ~ 0.9 and slightly depends on temperature, while the superposition of the reduced conductivity at all temperatures shows that the relaxation mechanism is temperature independent. Data have been analysed in the modulus formalism with a distribution of relaxation times using KWW stretched exponential function. The stretching exponent, β , is found to depend on temperature. The analysis of the temperature variation of the M'' peak indicates that the observed relaxation process is thermally activated. The inferences drawn from the above analysis (1) Arrhenius dependence of relaxation peak on temperature and (2) comparable values of activation energy obtained from conductivity and modulus analysis suggest that the ion transport in the investigated materials follows the hopping mechanism.

References

1. Garcia-Belmonte G, Bisquert J (2004) J Non-Cryst Solids 337 (3):272
2. Dyre JC, Schröder TB (2000) Rev Modern Phys 72(3):873
3. Funke K, Roling B, Lange M (1998) Solid State Ion 105(1–4):195
4. Ingram MD, Jean Robertson AH (1997) Solid State Ion 94(1–4):49
5. Bunde A, Ingram MD, Maass P (1994) J Non-Cryst Solids 172–174(2):1222
6. Vogel M (2004) Phys Rev B 70(9):094302
7. Prasada Rao R, Tho TD, Adams S (2009) J Power Sources 189 (1):385
8. Tho TD, Prasada Rao R, Adams S (2010) Solid State Electrochem (this issue)
9. Almond DP, West AR (1983) Solid State Ion 9–10:277
10. Funke K, Banhatti RD (2006) Solid State Ion 177:1551
11. Ngai KL, Rajagopal AK, Teitler S (1988) J Chem Phys 88:5086
12. Funke K (1993) Prog Solid State Chem 22:111
13. Roling B, Happe A, Funke K, Ingram MD (1997) Phys Rev Lett 78:2160
14. Anantha PS, Hariharan K (2005) Mat Chem Phys 89:428
15. Bhide A, Hariharan K (2007) Mat Chem Phys 105:213
16. Leo CJ, Subba Rao G, Chowdari BVR (2002) J Mat Chem 12:1848